

## Correlations Between Grain Boundary Structure and Energy\*

K.L. Merkle and D. Wolf

Materials Science Division  
Argonne National Laboratory, Argonne, IL 60439

The submitted manuscript has been authored  
by a contractor of the U.S. Government under  
contract No. W-31-109-ENG-38. Accordingly,  
the U.S. Government retains a nonexclusive,  
royalty-free license to publish or reproduce the  
published form of this contribution, or allow  
others to do so, for U.S. Government purposes.

## DISCLAIMER

This report was prepared as an account of work sponsored by an agency of the United States Government. Neither the United States Government nor any agency thereof, nor any of their employees, makes any warranty, express or implied, or assumes any legal liability or responsibility for the accuracy, completeness, or usefulness of any information, apparatus, product, or process disclosed, or represents that its use would not infringe privately owned rights. Reference herein to any specific commercial product, process, or service by trade name, trademark, manufacturer, or otherwise does not necessarily constitute or imply its endorsement, recommendation, or favoring by the United States Government or any agency thereof. The views and opinions of authors expressed herein do not necessarily state or reflect those of the United States Government or any agency thereof.

---

\*Work supported by the U.S. Department of Energy, BES-Materials Sciences,  
under Contract No. W-31-109-Eng-38.

Manuscript submitted to the *International Symposium on Metal/Ceramic  
Interfaces*, Irsee, Germany, June 30-July 5, 1991.

MASTER  
DISTRIBUTION OF THIS DOCUMENT IS UNLIMITED *do*

## **DISCLAIMER**

**This report was prepared as an account of work sponsored by an agency of the United States Government. Neither the United States Government nor any agency thereof, nor any of their employees, makes any warranty, express or implied, or assumes any legal liability or responsibility for the accuracy, completeness, or usefulness of any information, apparatus, product, or process disclosed, or represents that its use would not infringe privately owned rights. Reference herein to any specific commercial product, process, or service by trade name, trademark, manufacturer, or otherwise does not necessarily constitute or imply its endorsement, recommendation, or favoring by the United States Government or any agency thereof. The views and opinions of authors expressed herein do not necessarily state or reflect those of the United States Government or any agency thereof.**

---

## **DISCLAIMER**

**Portions of this document may be illegible in electronic image products. Images are produced from the best available original document.**

# CORRELATIONS BETWEEN GRAIN BOUNDARY STRUCTURE AND ENERGY

K. L. MERKLE and D. WOLF

Materials Science Division, Argonne National Laboratory, Argonne, IL 60439

## ABSTRACT

High-resolution electron-microscopy (HREM) and computer simulations of  $\langle 110 \rangle$  tilt grain boundaries (GBs) in Au are used to investigate correlations between atomic-scale GB structure and energy. The energies calculated for a variety of symmetric and asymmetric GBs suggest that asymmetric GB-plane orientations are often preferred over symmetric ones. The experimentally observed faceting behavior agrees with the computed energies. Computer simulations indicate general interrelations between GB energy and (i) volume expansion and (ii) the number of broken bonds per unit area of GB. These atomic-scale microstructural GB parameters, as evaluated from HREM observations, are compared to simulation results.

## 1. INTRODUCTION

It is not surprising that polycrystalline materials generally contain a wide variety of grain boundaries (GBs), since there are five macroscopic degrees of freedom for the formation of a single planar interface between two crystals. From the range of geometries the subset of low-energy high-angle GBs largely determines the naturally occurring boundaries and has often been a subject of investigation. Since it is difficult to assess the geometry of the internal interfaces between the crystallites in a polycrystal, rarely has a full geometric characterization of the boundaries in a polycrystal been possible, even on the macroscopic scale. Simulations or model studies of GBs have typically also been limited to simple interfacial geometries, such as symmetric GB-plane orientations. Moreover, in order to study the true nature of an interface, the GB has to be studied at the atomic level. Experimentally this is possible for tilt GBs by HREM, which not only allows the observation of possible microfacets on the atomic scale, but will also give information on the rigid-body displacements as well as the local coordination of atomic columns across the GB.

Asymmetric GBs, i. e., interfaces made up of two crystallographically different sets of planes, are often found experimentally, and their importance has been suggested (a) from high-resolution electron microscopy (HREM) studies [1, 2] and (b) based on theoretical considerations [3- 5]. Recently computer simulations have been used to determine the energies of a variety GBs in fcc and bcc metals, including symmetric [6, 7] and asymmetric tilt and twist (i.e., general) boundaries [4, 8, 9].

In the present investigations HREM observations are combined with computer simulations to study symmetric and asymmetric tilt GBs in Au bicrystals. In each bicrystal, the relative orientation of the crystals is fixed, however the GB plane is free to choose any symmetric or asymmetric inclination. Simulations are performed for a variety of symmetric and asymmetric GBs and comparisons are made to observed facets, volume expansion (i. e. the normal component of the rigid-body translation) and the local atomic environments in the GBs.

## 2. GEOMETRIC CHARACTERIZATION OF GRAIN BOUNDARIES

The misorientation between the two grains of a bicrystal is defined by a misorientation axis  $\hat{n}_r$  (in the present experiments  $\langle 110 \rangle$ ) and a misorientation angle  $\psi$ . Within this bicrystal tilt GBs can be formed, subject to the constraint that  $(\hat{n}_1 \cdot \hat{n}_r) = (\hat{n}_2 \cdot \hat{n}_r) = 0$ , where  $\hat{n}_1$  and  $\hat{n}_2$  are the GB plane normals in crystals 1 and 2, respectively. Therefore, as illustrated in fig.1, one additional parameter, conveniently defined as the inclination  $\alpha$ , is sufficient to characterize the GB plane within a tilt bicrystal. We note that at most two different *symmetric* tilt GBs are formed, whereas geometrically there exists the possibility to form infinitely many asymmetric tilt GBs. Figure 1(a), however, clearly suggests that there is a finite number of facets which are preferred. The individual GBs (facets) are best characterized by specifying the pairs of crystallographic planes that form the GB,  $(h k l)_1$  and  $(h k l)_2$ . All general boundaries on these planes (involving twist and tilt components) are then formed by twist rotations around the GB plane normal by some angle  $\theta$ . This procedure has been found to be very useful in simulating a wide range of GB geometries [4-7].

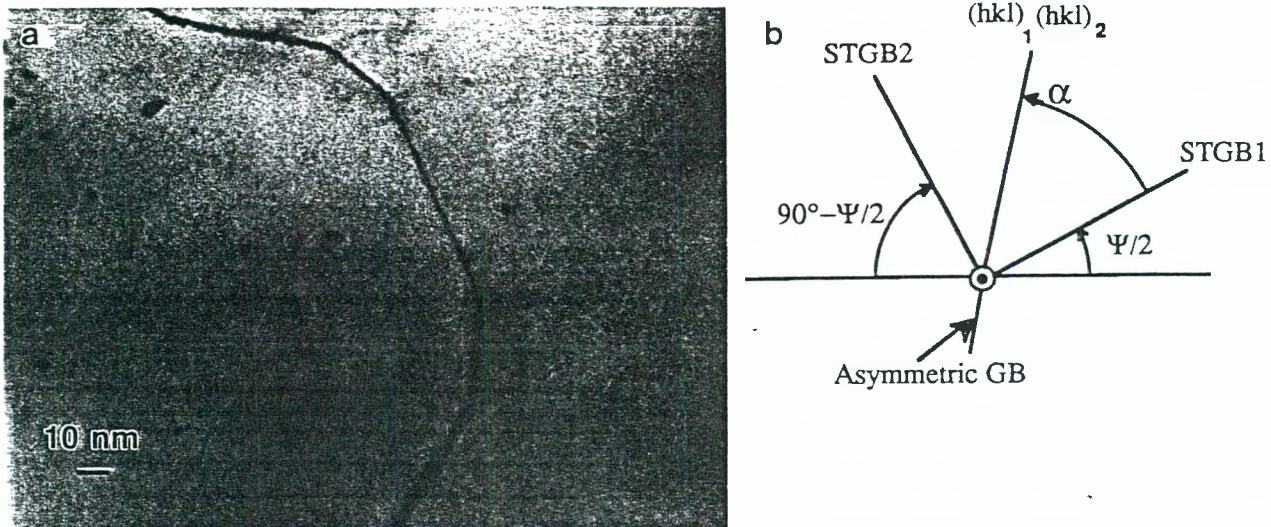


Fig. 1. (a) Transmission electron micrograph of  $<1\bar{1}0>$  tilt GBs in Au, viewed edge-on. (b) Different facets are characterized by their inclination  $\alpha$ ; for a twofold axis symmetric GBs are at  $\alpha=0^\circ$  (STGB1) and  $\alpha=90^\circ$  (STGB2).

### 3. GRAIN BOUNDARY SIMULATIONS

A zero-temperature iterative energy-minimization algorithm ("lattice statics") was used to compute the fully relaxed atomic structures and energies of various symmetric and asymmetric GBs. To enable the GB to expand or contract, the unit-cell volume was allowed to increase or decrease in response to the internal pressure [10]. Also, by computing the forces which the two halves of the bicrystal exert on each-other, translations parallel to the GB plane were allowed while the atoms relax. By starting from a variety of initial rigid-body translational configurations, the GB energy is thus minimized with respect to both the atomic positions and the three translational ("microscopic") degrees of freedom of the GB.

A many-body potential of the embedded-atom-method (EAM) type, fitted for Au [11], was employed, enabling a direct comparison with the HREM experiments. A comparison of these simulations to those obtained with a much simpler Lennard-Jones potential suggests that qualitatively, the main results are typical of fcc metals, while smaller differences may well occur from one material to another [12].

A typical result of a series of simulations is illustrated in fig. 2 which shows the general (i.e., asymmetrical twist) boundaries formed by the (557) and (771) planes for different twist angles  $\theta$ . For any combination of planes it is found that the two asymmetric *tilt* GB configurations at  $\theta=0^\circ$  and  $\theta=180^\circ$  give rise to pronounced energy cusps (see fig. 2). These cusps are thought to be due to the relatively small planar unit-cell areas of these boundaries which enable a rather good interlocking of the atom positions across the GB [7, 9]. By comparison, the general boundaries obtained for arbitrary values of  $\theta$ , with both tilt and twist components, have relatively large planar unit cells. The energy cusps associated with the asymmetric *tilt* GB configurations point to the importance of tilt GBs (symmetrical and asymmetrical) in polycrystalline materials. Fortunately, these GBs are the types of boundaries which can be investigated by means of atomic-scale HREM.

### 4. HIGH-RESOLUTION ELECTRON MICROSCOPY OF TILT GRAIN BOUNDARIES

Thin (110) gold films were grown epitaxially on NaCl in a UHV system and then pairwise sintered together at the appropriate misorientation angle, using a modification of the Schober-Balluffi technique [13]. After removal from the NaCl substrate, columnar grains with the desired tilt GBs were obtained by further annealing. Suitably thin samples for HREM were obtained by ion-beam milling. Typically, high-resolution images were taken under axial illumination at a magnification of 700,000 X for several defocus values near optimum defocus, utilizing a H9000 high-resolution electron microscope, operated at 300 kV.

Upon annealing, the GBs were constrained to the vertical orientation in the films while forming pure tilt GBs, based on the minimization of energy by GB-area reduction. However, the GBs were free to choose any tilt GB inclination. All of the bicrystals examined were found to exhibit a number of facets, corresponding to a finite set of inclination angles  $\alpha$ . Frequently island grains

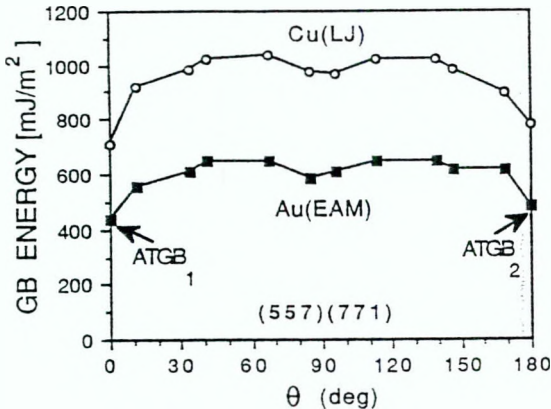


Fig. 2 Energies as a function of twist angle  $\theta$  for (557)(771) asymmetric twist GBs. Note deep cusps at the tilt configurations,  $\theta = 0^\circ$  and  $\theta = 180^\circ$ .

were also present, surrounded by a single-crystalline matrix. Such structures can in principle give information on relative GB energies from the length and frequency of observed facets. However, typically no clearly dominant facets were apparent, except for misorientations where facets of particularly low-energy, such as the coherent twin and the (113)(113) symmetric tilt GB, or the (111)(001) asymmetric tilt GB, could be formed.

In order to be able to distinguish whether the facets are planar on an atomic scale, or whether the interface reconstructs into smaller, atomic-scale facets, it is important to make the observations at a spatial resolution close to the atomic level. An illustration of microfaceting is given in fig. 3, which shows the decomposition of a GB into asymmetric facets bounded by dense-packed planes. The observed planar facets presumably are those associated with low interfacial energies. While a number of  $<110>$  bicrystals were investigated, detailed comparisons between simulated and observed boundaries were performed for the  $\Sigma=9$  and  $\Sigma=11$  systems, where  $\Sigma$  is the reciprocal coincident-site-lattice density.

## 5. DEPENDENCE OF GRAIN BOUNDARY ENERGY ON INCLINATION

Given two grains at a specified misorientation, it is of considerable importance to find the GB planes with low interfacial energy, since they will largely determine the faceting behavior in polycrystalline materials. Simulation results in fig. 4 show GB energies (for the Au(EAM) potential) as a function of inclination angle,  $\alpha$ , for the  $\Sigma=9$  and  $\Sigma=11$  bicrystals. Among the particular combinations of GB planes considered in the figure, only the (112)(1,1,22) GB has not been observed experimentally. Several points should be noted about fig. 4: (i) The majority of GB energies lie in a relatively narrow band. (ii) For those facets that have been observed experimentally, the data points in fig. 4 must represent energy cusps. (iii) Symmetric GBs, corresponding to the inclinations  $\alpha=0^\circ$  and  $\alpha=90^\circ$ , are not necessarily preferred energetically. The experimentally observed faceting behavior in  $\Sigma=9$  and  $\Sigma=11$  Au bicrystals shows good agreement with the calculated energies [14]. The fact that many, often asymmetric facets are present is thus in agreement with calculated GB energies.

The rather similar energies associated with different inclinations explains the multitude of facets that have been observed in these and other bicrystals. While the actual number of low-energy boundaries may vary with misorientation and may include quite low-energy symmetric GBs, such as (113)(113) for  $\Sigma=11$  bicrystals, it is clear that tilt bicrystals are not dominated by symmetric facets. In fact, because in contrast to the geometrically unlimited number of possible asymmetric configurations, at most two different symmetric GBs are possible for each misorientation [14], asymmetric GBs may, indeed, be expected to play a dominant role in polycrystalline samples. Moreover, kinetic factors may favor the growth of asymmetric boundaries in annealed polycrystals. Dissociation of asymmetric facets into *symmetric* facets has only been observed when  $\Sigma=3$  coherent twin boundaries can be formed; similarly *asymmetric* microfacetting can occur when two dissimilar low-index (i.e. atomically dense-packed) planes are close to being parallel in the two grains (see fig. 3).

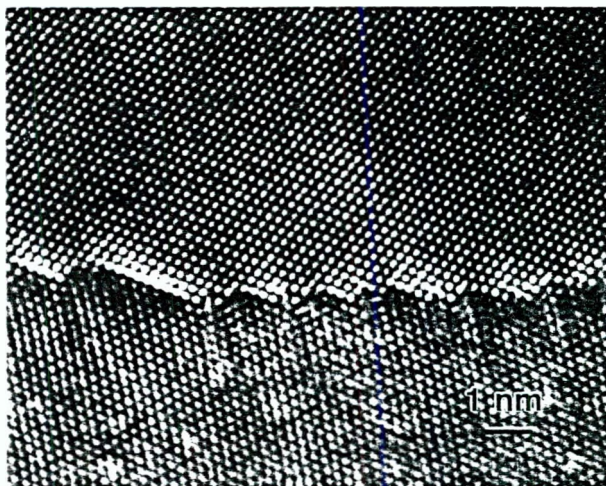


Fig. 3 HREM micrograph of (225)(441) GB, which disintegrates into (111)(001) asymmetric microfacets.

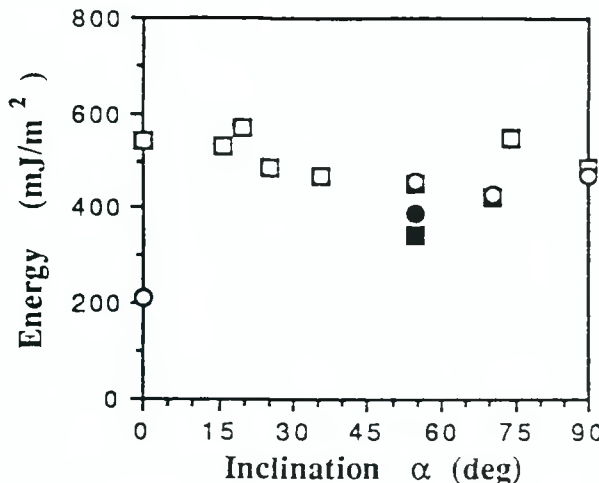


Fig. 4. Calculated Au (EAM) GB energies as a function of inclination  $\alpha$  for  $\Sigma=9$  (□) and  $\Sigma=11$  (○) bicrystals. Full symbols indicate GB-energy reduction due to dissociation .

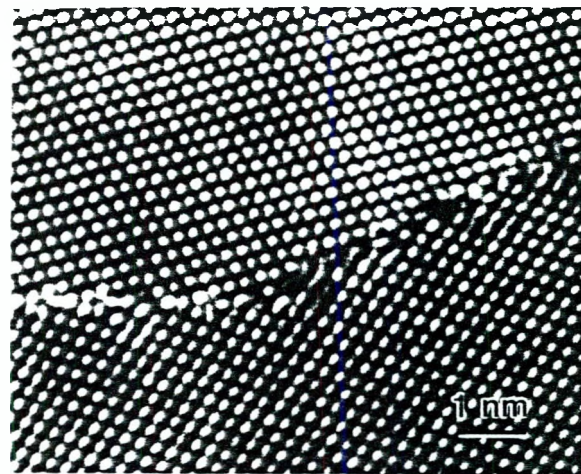


Fig. 5. Symmetric and asymmetric facets coexist in this HREM micrograph of <110> tilt GB in Au,  $\psi=39^\circ$ . (221)(221) GB at left goes over into asymmetric (557)(771) facet.

## 6. STRUCTURE-ENERGY CORRELATIONS

The rigid-body displacements have long been known to provide an important relaxation mechanism for minimization of the energies of GBs. A direct relationship between GB energy and the normal component of the rigid-body displacement, the volume expansion, had been suggested more than 30 years ago by Seeger and Schottky [15]. More recently detailed atomistic simulations of a wide range of GB geometries in metals have shown a roughly linear relationship between GB energy and volume expansion (see fig. 6 (a)). Therefore, experimental measurements of this quantity should provide a direct indication of GB energy.

Experimentally it is difficult to measure volume expansions precisely because of their small magnitudes, typically only a small fraction of a lattice parameter. Lattice fringe techniques have however recently been developed that should provide a precision of better than 0.01 nm [16, 17]. As illustrated in fig. 7, compared to the simulation results, the measured volume expansions for Au are typically greater by more than a factor of two, except for the (111)(111) twin which shows practically zero expansion. The origin of this discrepancy is not clear at present,

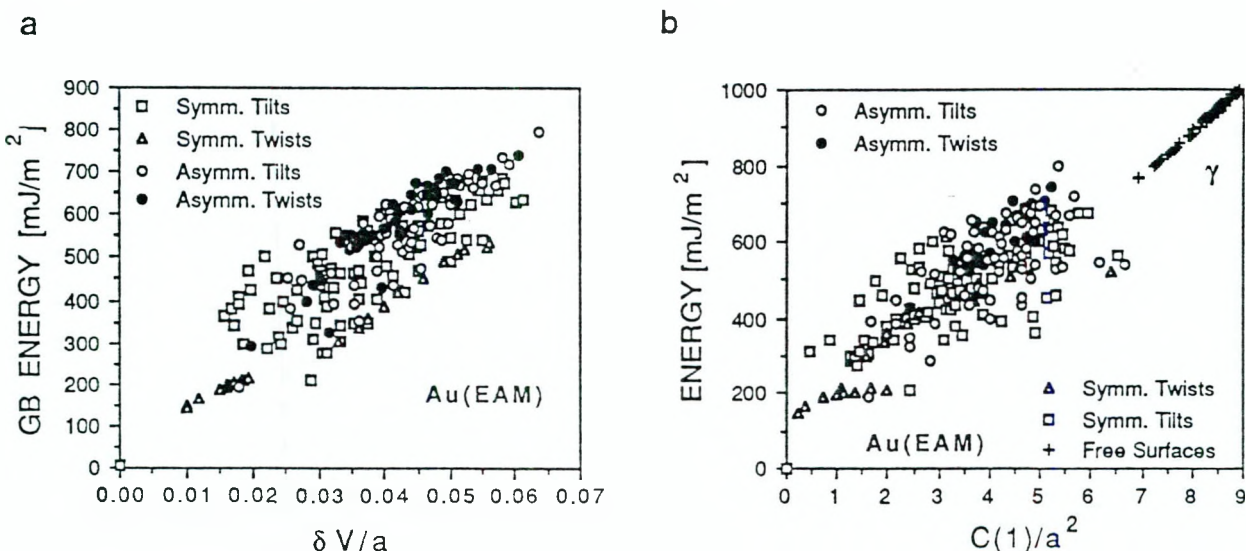


Figure 6. (a) Correlation between the GB energy and volume expansion per unit GB area,  $\delta V/a$  (in units of the lattice parameter  $a$ ) for symmetrical and asymmetrical tilt and twist GBs in fcc metals calculated for Au(EAM) potential. (b) GB energy vs. coordination coefficient  $C(1)$ . (The number of broken nearest-neighbor bonds per unit area is given by  $C(1)/2$  ).

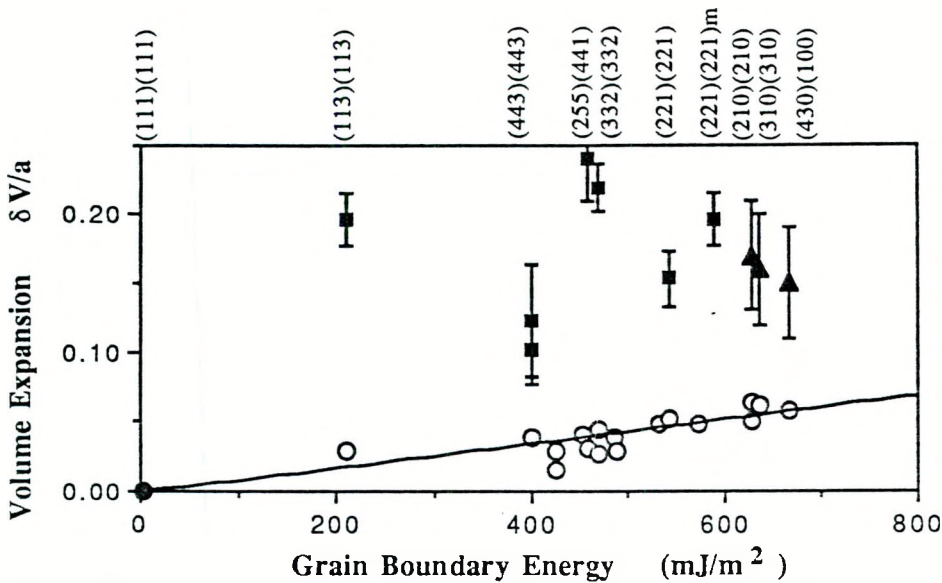


Fig. 7. Measured (full symbols) and calculated (open symbols) volume expansions displayed against calculated GB (EAM) energies. Triangles are measurements of  $\Sigma = 5$  grain boundaries in Au from ref. [18]. The error bars in the present measurements represent standard deviations from several measurements of the same interface. The GBs are identified at the top of the figure.

but may in part be due to problems with the Au (EAM) potential. Also, the three highest values of  $\delta V$  in fig. 7 were obtained for a small island grain, for which the GB relaxations may have been constrained. Although in principle  $\delta V$  values can now be investigated systematically by the HREM technique, much work remains to be done to establish correlations to the different GB structures, including their chemical composition.

HREM observations of ceramic and metallic GBs also suggested that the degree of atomic matching at the GB is correlated to GB energy, since, as for the preference of dense-packed planes, extended facets also are observed when a particularly good match can be accomplished between atomic planes crossing the GB. Recent atomistic simulations have in fact shown that in terms of the cumulative atomic miscoordination around each atom there is a good correlation between the number of "broken bonds" per GB unit area and GB energy (see fig 6 b) [19].

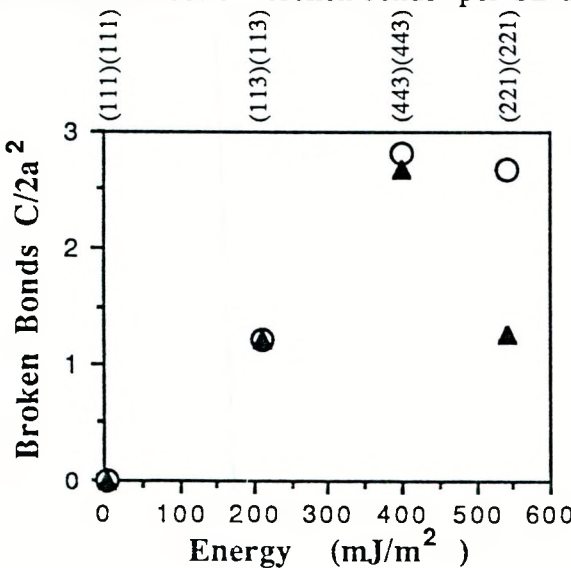


Fig. 8. Measured ( $\blacktriangle$ ) and calculated ( $\circ$ ) coordination coefficients (broken bonds per unit GB area) vs. GB energy.

Although the HREM technique gives at best a two-dimensional projection of the atomic structure and therefore requires observations along more than one zone axis for a three-dimensional reconstruction of a GB, one can attempt to construct three-dimensional models of tilt GBs based on the assumption that there are no shifts along the direction of observation. Using this simple model, we have analyzed HREM images in terms of the number of broken bonds per unit GB area.

By determining the number of atoms within a shell that bisects the distance between first- and second-nearest neighbors in the ideal lattice, the number of broken bonds can be found for each atom  $n$  within the GB structural unit as the deviation  $\Delta K_n = K_n - K_{id}$  from the perfect fcc crystal coordination number,  $K_{id}=12$ . A coordination coefficient  $C = 1/A \sum_n |\Delta K_n - \langle \Delta K \rangle|$ , where  $A$  is GB unit area and the sum is performed over all

atoms in the GB unit cell [19]. The number of broken bonds per GB unit area is given by  $C/2$ , as plotted in fig. 8 for several symmetric  $\langle 1\bar{1}0 \rangle$  tilt GBs in Au and shows a close to linear relationship to the calculated EAM energies for these boundaries. Moreover it is seen that the agreement between the miscoordination coefficients from experiment and simulations is quite good.

## 7. SUMMARY AND CONCLUSIONS

HREM experiments provide valuable information on several atomic-scale GB parameters. The fact that for each bicrystal (a) many more asymmetric combinations of GB planes are possible than symmetric ones, and (b) asymmetric tilt GBs often have lower energies than symmetric tilt GBs, suggests a special importance of asymmetric GBs in polycrystalline materials. Moreover, from the frequent observations of facets in which low-index planes are combined, it appears that relaxations towards GB structures formed by combination of two low-index planes can create asymmetric GBs with a particularly low energy. Asymmetric GBs may be of considerable importance in grain growth, diffusion induced GB migration, and other GB properties.

Extensive simulations for GBs in fcc and bcc metals, using both pair- and many-body potentials, demonstrate a practically linear relationship between the energy and volume expansion per unit GB area. Combined with the simulations, HREM measurements of the volume expansion thus provide direct information on the GB energy, while a comparison of measured with computed rigid-body translations parallel to the boundary plane provide an important test for (i) the validity of the interatomic potential and (ii) the relaxation procedures used in the simulations.

Finally, HREM experiments clearly demonstrate a tendency of the *atomic* structure to preserve a high degree of atomic-level coherency across the interface. The underlying causes, elucidated via simulation, are closely connected with the desire of the interface to minimize its number of broken bonds, i.e. its energy.

## ACKNOWLEDGEMENTS

This work was supported by the U.S. Department of Energy, Basic Energy Sciences, under contract W-31-109-Eng-38. The Department of Materials Science & Engineering at Northwestern University is gratefully acknowledged for making the H9000 available for this research.

## REFERENCES

1. K. L. Merkle, J. F. Reddy, C. L. Wiley and D. J. Smith, in **Ceramic Microstructures '86**, edited by Pask and Evans (Plenum 1987) p. 241.
2. K. L. Merkle and D. J. Smith, *Ultramicroscopy* **22**, 57 (1987).
3. D. Wolf, *Mat. Res. Soc. Symp. Proc.* **40**, (1985).
4. D. Wolf in, **Ceramic Microstructures '86, Role of Interfaces**, edited by J. A. Pask and A. G. Evans (Plenum 1987) p. 177.
5. D. Wolf and S. Phillpot, *Mater. Sci. Eng. A* **107**, 3 (1989).
6. D. Wolf, *Acta Metall.* **37**, 1983 (1989).
7. D. Wolf, *Acta Metall. Mater.* **38**, 781 (1990).
8. A. P. Sutton, *Mat. Res. Soc. Proc.* **122**, 81 (1988).
9. D. Wolf, *Acta Metall. Mater.* **38**, 791 (1990).
10. D. Wolf, *Acta Metall.* **37**, 1983 (1989), *J. Appl. Phys.* **69**, 185 (1991).
11. S. M. Foiles, M. I. Baskes and M. S. Daw, *Phys. Rev. B* **33**, 7983 (1986).
12. D. Wolf, J. Lutsko and M. Kluge, in **Atomistic Simulation of Materials**, edited by V. Vitek and D. J. Srolovitz (Plenum 1989) p. 245.
13. T. Schober and R. W. Balluffi, *Phil. Mag.* **21**, 109 (1970).
14. K. L. Merkle and D. Wolf, *Phil. Mag.*, in press.
15. A. Seeger and G. Schottky, *Acta Met.* **7**, 495 (1959).
16. G. J. Wood, W. M. Stobbs and D. J. Smith, *Phil. Mag. A* **50**, 375 (1984).
17. K. L. Merkle, submitted to *Ultramicroscopy*.
18. F. Cosandey, S.-W. Chan and P. Stadelmann, *Colloque de Phys.* **51**, C1-109 (1990).
19. D. Wolf, *J. Appl. Phys.* **68**, 3221 (1990).